Transactions of the 15th International Conference on
Structural Mechanics in Reactor Technology (SMiRT-15)
Seoul, Korea, August 15-20, 1999

Time History Non-Linear Earthquake Response Analysis Considering Materials and Geometrical Non-Linearity

Toshio Kobayashi[1], Kazuhide Yoshikawa[2], Eiji Takaoka[2], Masaaki Nakazawa[3] and Yasuhiro Shikama[3]

1) Kajima Technical Research Institute, Japan
2) Kajima Corporation, Japan
3) Tokyo Electric Power Company, Japan

ABSTRACT

A time history nonlinear earthquake response analysis method was proposed and applied to earthquake response prediction analysis for a Large Scale Seismic Test Program in Hualien, Taiwan, in which a 1/4 scale model of a nuclear reactor containment structure was constructed on sandy gravel layer. In the analysis both of strain-dependent material nonlinearity, and geometrical nonlinearity by base mat uplift,were considered. The "Lattice Model" for the soil-structure interaction model was employed. An earthquake record on soil surface at the site was used as control motion, and deconvoluted to the input motion of the analysis model at GL-52 m with 300 Gal of maximum acceleration. The following two analyses were considered: (A) time history nonlinear, (B) equivalent linear, and the advantage of time history nonlinear earthquake response analysis method is discussed.

1. INTRODUCTION

A Large Scale Seismic Test (LSST) to study soil-structure interaction during earthquakes has been conducted on a 1/4-scale model nuclear reactor containment structure in Hualien, Taiwan, as an extension of the program in Lotung, under the control of an international consortium [1]. Fig.1 shows a section of the model.

After forced vibration tests using an exciter, observations commenced in May, 1993 to obtain high level earthquake-induced soil-structure interaction data with nonlinear characteristics. But these data have not been recorded yet.

A time history nonlinear earthquake response analysis method was proposed, in which both strain dependent material nonlinearity and geometrical nonlinearity by base mat uplift were considered The method was applied to a prediction analysis of the earthquake response of the Hualien model.

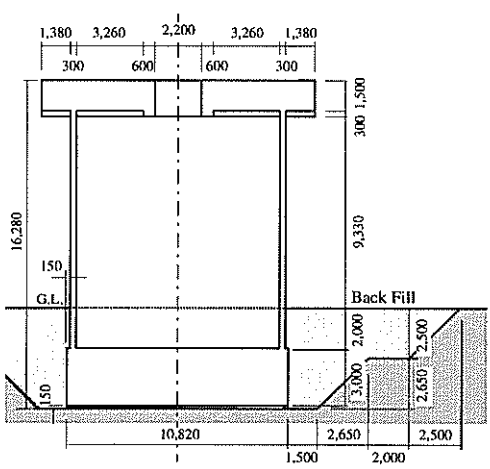

Fig. 1 Section of the model structure

2. MODEL STRUCTURE AND SOIL CONDITIONS

The test model is approximately 1/4-scale of commercial nuclear reactors in the USA, France, Taiwan,Korea and Japan. The diameter of the cylindrical shell portion of the model is 10 m, and its total height 16 m. The roof slab is 13 m in diameter, and 1.5 m in thickness, the foundation's diameter is 10 m, and its thickness 3 m. The model was made of reinforced concrete with a weight of about 1,400 tons. The cross section is shown in Fig.1. This structure was idealized into a mathematical multi-mass bending-shearing model, as shown in Fig. 2.

Soil properties and geometry at the Hualien site were investigated, and the results found to be of an axi-symmetric type, named a "Unified Model" as shown in Fig. 3 [2].

The shear wave velocity (Vs) of surface layer was about 200 m/sec by 5 m in depth; just beneath the base mat was Gravel 1 in which Vs = 383 m/sec, the outer region of the same level was Gravel 2 in which Vs = 333 m/sec, the deeper level was Gravel 3 in which Vs = 476 m/sec, and the backfill soil was Vs = 400 m/sec.

Strain-dependent material nonlinearity of rigidity and damping were investigated for each layer, as shown in Fig. 4.

3. BASIC THEORY

The "Lattice Model" was employed for a Soil-Structure Interaction model, in which surrounding soil was idealized by multi masses connected by lateral axial springs and vertical shearing springs, which represent local soil stiffness. The "Lattice Model" is shown in Fig. 5. The following two kinds of nonlinearity were considered :

Material Nonlinearity

Strain-dependent material nonlinearity was idealized by a Modified Ramberg-Osgood model, as shown in Eq. (1).

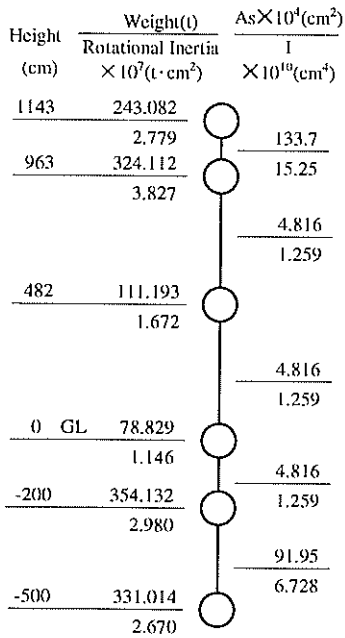

Fig. 2 Multi-Mass-Bending Shearing Model of Model Structure

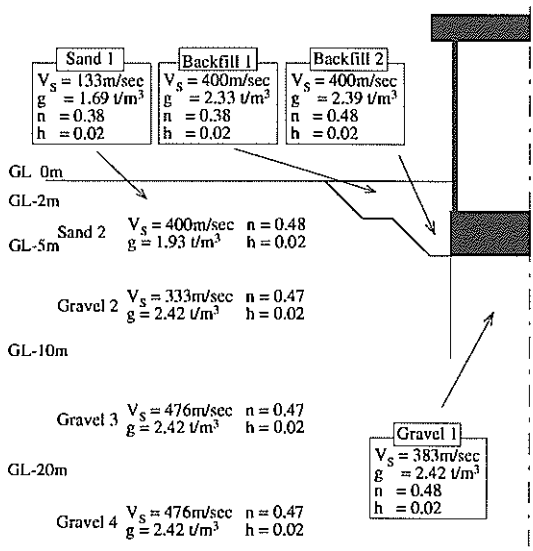

(after Okamoto et al [5])
Fig. 3 Unified Soil Model

$$\gamma = \left(\tau_y / G_0\right) \times S \times \left(1 + \alpha |S|^{\beta}\right) \qquad (1)$$

where, $G_0 = \tau_y / \gamma_y$, $S = \tau / \gamma_y$, $\beta = \dfrac{2\pi h_{ref}}{2\left(1 - Y_{ref}\right) - \pi h_{ref}}$, $\alpha = \dfrac{1 - Y_{ref}}{Y_{ref}} \times \left(\dfrac{\tau_y}{G_0}\right)^{\beta} \times \left(\dfrac{1}{Y_{ref} \times \gamma_{ref}}\right)^{\beta}$, $Y_{ref} = \dfrac{G_{ref}}{G_0}$, $\dfrac{\tau_y}{G_0} = \dfrac{1}{600}$

and γ_{ref}, G_{ref}/G_0, h_{ref} and τ_y are given from soil test results.

The general concept of the Modified Ramberg-Osgood model is shown in Fig.6.

Geometrical Nonlinearity

The rocking stiffness of supporting soil was idealized by a fiber model. Each fiber consists of a gap element and a soil spring element. The gap element transmits no tensile stress which can express the geometrical nonlinearity of base mat uplift. The soil spring element also have Ramberg-Osgood characteristics. The general concept of the fiber model is shown in Fig.7.

The equilibrium equation at the base mat bottom is given in Eq. (2) in incremental form by vertical displacement (v) and rocking angle (θ) at the base mat center under a rigid base assumption.

$$\begin{Bmatrix} \Delta N \\ \Delta M \end{Bmatrix} = \begin{bmatrix} K_V & K_{VX} \\ K_{VX} & K_{VX2} \end{bmatrix} \begin{Bmatrix} \Delta v \\ \Delta \theta \end{Bmatrix} \qquad (2)$$

where, $K_V = \sum_{i=1}^{n} kv_i$, $K_{VX} = \sum_{i=1}^{n} kv_i \times x_i$, $K_{VX2} = \sum_{i=1}^{n} kv_i \times x_i^2$, N ; vertical force, M : overturning moment,

kv_i: rigidity of fiber model, $kv_i = kv \times A_i$, A_i : Area of i-th fiber model, $kv = K_\theta / I$,

K_θ : Rotational rigidity of supporting soil obtained by axi-symmetric FEM

I : Moment of inertia of base mat area

x_i : distance between fiber model and base mat center.

Mesh layout of fiber model is shown in Fig.8.

4. EARTHQUAKE RESPONSE ANALYSIS OF THE HUALIEN LSST MODEL

Input Earthquake

Observed record of January 20, 1994 earthquake on the free soil surface point at the Hualien site, named A15, 56.46 m from the model center, was employed as the control motion. Its maximun accleration was 32.1 Gal.

Input motion for the analysis model at GL-52.6 m was deconvoluted from the record using the "SHAKE", normalized at 300 Gal as maximum acceleration. The acceleration time history and response spectrum of the model input earthquake at GL-52.6 m are shown in Fig.9.

Analysis Case

To clarify the characteristics of the proposed method, the following two cases were analysed:

(A) Time history nonlinear analysis with both strain-dependent material nonlinearity and geometrical nonlinearity by base mat uplift.

(B) Equivalent linear analysis with strain-dependent soil rigidity and damping based on SHAKE results.

Analysis Results

(i) The acceleration time history and response spectrum at free soil surface are shown in Fig.10. Case (A) contains high frequency components during all time ranges, compared with Case (B). The high frequency components of the first 14 seconds are amplified by 2 from input motion in Case (A). This is because the input motion level is low in the first 14

seconds, soil response is almost in linear range, and consequently high frequency components were amplified.

After 14 seconds in Case (A), the response level is reduced to smaller than the input motion level. During this time, the input level increases and the soil characteristics show nonlinearity in low rigidity and high damping.

In the response spectra, there are several peaks in Case (A) in the period range smaller than 0.1 second, but not in Case (B). The response spectra of Case (B) is larger than that of Case (A) in the period range larger than 0.15 sec, and opposite in the period range smaller than 0.15 sec. Case (A) expressed the change of frequency transfer characteristics of the soil-structure interaction system, depending on input level during an earthquake.

(ii) Fig.11 compares the maximum response acceleration distribution of the model and soil columns of cases (A) and (B). Soil column response is almost the same for both cases. The mass inertia effect of the model structure is small, compared with soil mass. The values were 150 ~ 200 Gal lower than -12 m for both Case (A) and (B). At the soil surface, the response acceleration of Case (B) is larger than that of Case (A).

(iii) Maximum response shear strain distribution of soil columns is shown in Fig. 12 comparing cases (A) and (B). Both cases show almost the same results, and the maximum values are about 1.0×10^{-3}.

(iv) Hysteresis loops of overturning moment and the rotational angle of the base mat are shown in Fig.13 comparing cases (A) and (B). Changes in stiffness and damping are observed in Case (A). As the result, there is not uplift phenomena at the base mat bottom in Case (A), while the ratio of the compression area to the whole base mat area is 56%, calculated from the maximum overturning moment given in Case (B) and the axial force of gravity, with the assumption that supporting soil transmit no tensile stress.

(v) Rotational angle acceleration time histories and response spectra are shown in Fig.14 comparing cases (A) and (B). The peak value of Case (B) in response spectra at 0.2 sec is larger than in Case (A), but the other range Case (A) are lager.

(vi) Acceleration time history and response spectra on the roof are shown in Fig.15 comparing cases (A) and (B). The peak value of Case (B) in a response spectra of 0.2 sec is larger than in Case (A), but the other ranges in both Cases reveal almost the same level.

5. CONCLUSION

Earthquake response analysis was conducted on the Hualien project using the record of an earthquake at the site, normalized 300 Gal at GL-52 m. In comparisons between Case (A) : time history nonlinear analysis, and Case (B) : equivalent linear analysis, the following conclusions were drawn.

(a) Maximum response acceleration of the model in Case (A) was small compared to that in Case (B).

(b) The peak response spectra in Case (A) were wide and low, compared to those in Case (B).

(c) There were no uplift phenomena at the base mat bottom in Case (A), while the minimum ratio of the compression aria to whole base mat area is 56 % in Case (B).

REFERENCES

1. Tang, H. T., Stepp, J. C., Cheng, Y. H., Yeh, Y. S., Nishi, K., Iwatate, T., Kokusho, T., Morishita, H., Shirasaka, Y., Gantenbein, F., Touret, J. P., Sollogoub, P., Graves, H. & Costello, J. 1991. The Hualien large-scale seismic test for soil-structure interaction research. Proc. 11 th SMiRT: K04/4. Tokyo, Japan.

2. Okamoto, T., Kokusho, T., Tanaka, Y., Kudo, K. & Kawai, T. 1995. Ground model for seismic response analysis in Hualien project of large scale seismic test. Proc. 13th SMiRT, Vol. III: pp. 103-108.

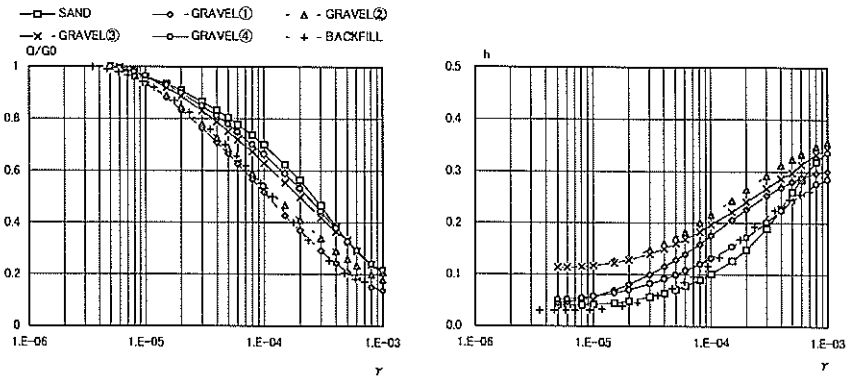

(a) Rigidity (b) Damping

Fig.4 Strain Dependent Material Non-linearity

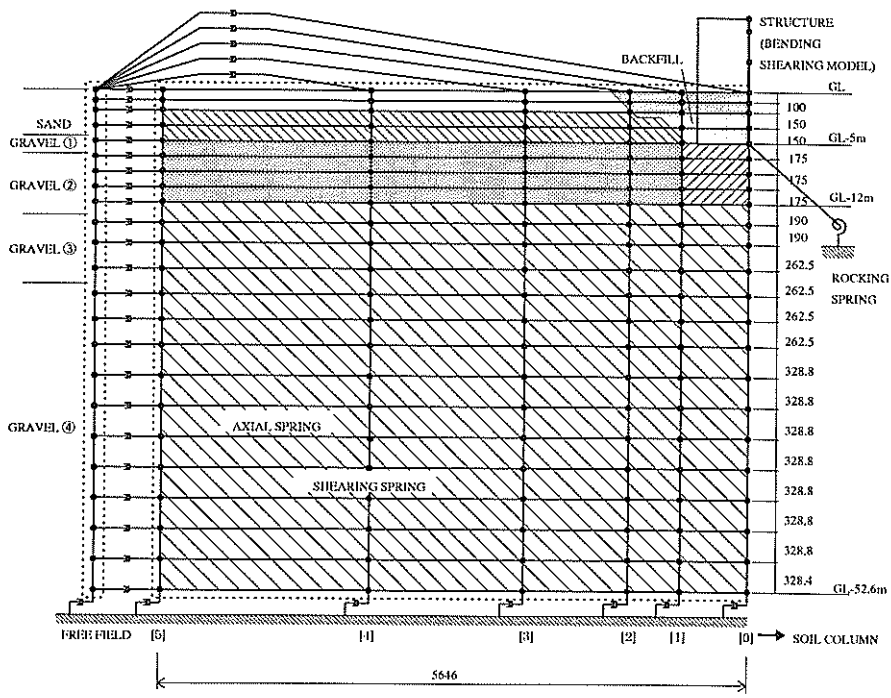

Fig.5 Lattice Model

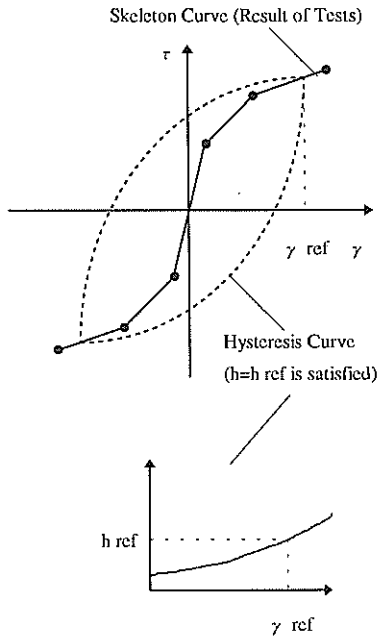

Fig.6 General Concept of Modified Ramberg-Osgood Model

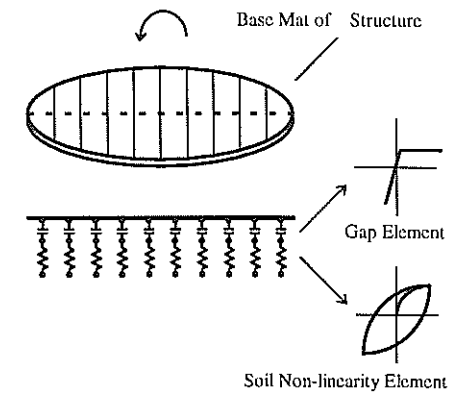

Fig.7 General Concept of Fiber Model

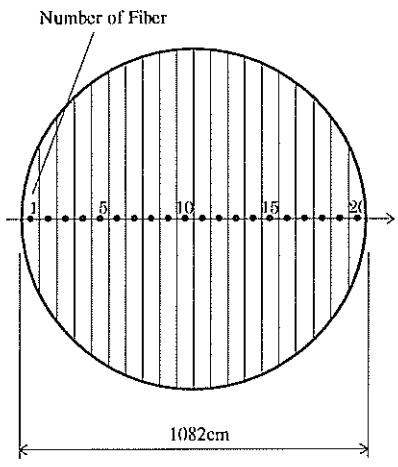

Fig.8 Mesh Layout of Fiber Model

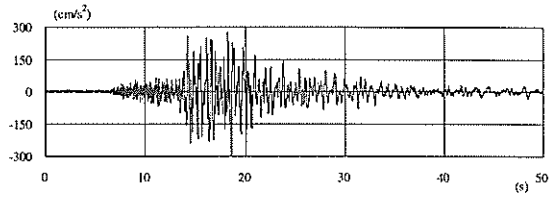

(a) Acceleration Time History

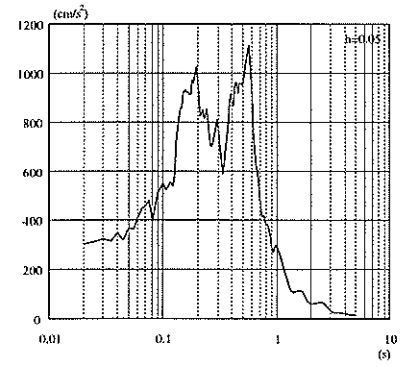

(b) Response Spectrum

Fig.9 Input Earthquake at GL-52.6m

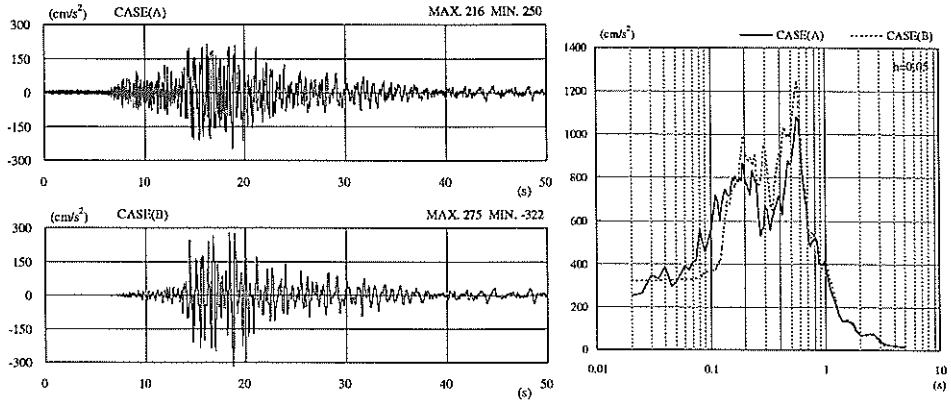

(a) Acceleration Time Histories (b) Response Spectra

Fig.10 Response on Free Soil Surface

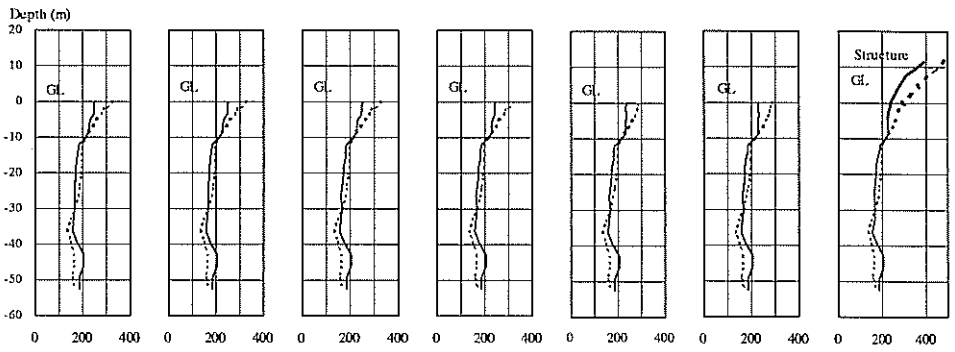

Fig.11 Maximum Response Acceleration Distribution

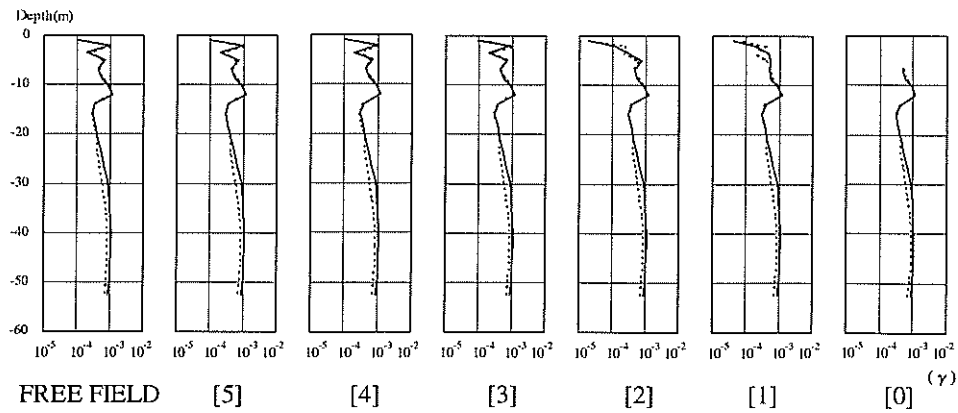

Fig.12 Maximum Response Shear Strain Distribution

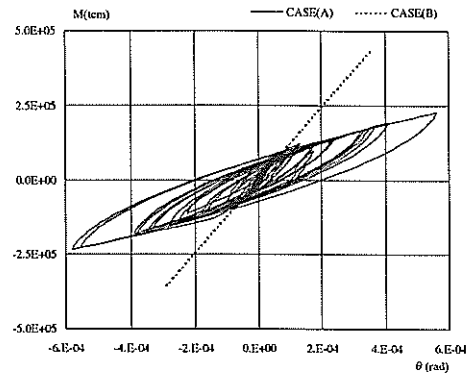

Fig.13 Hysteresis loops of Overturning Moment and Rotational Angle of Base Mat

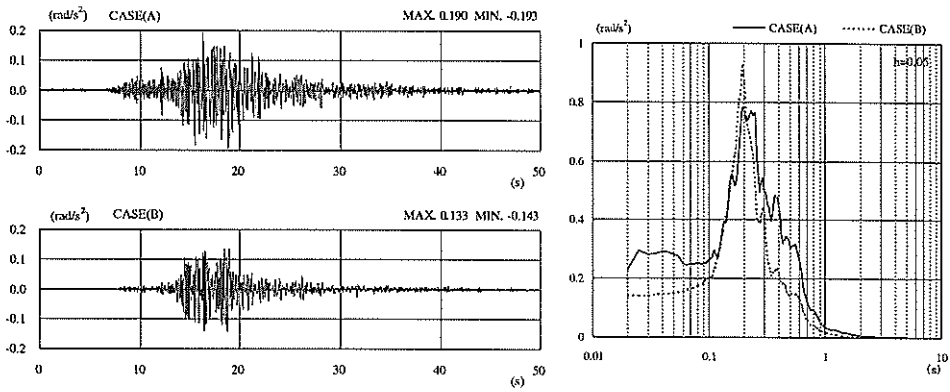

(a) Rotational Angle Acceleration Time Histories (b) Response Spectra

Fig.14 Response of Base Mat Rotation

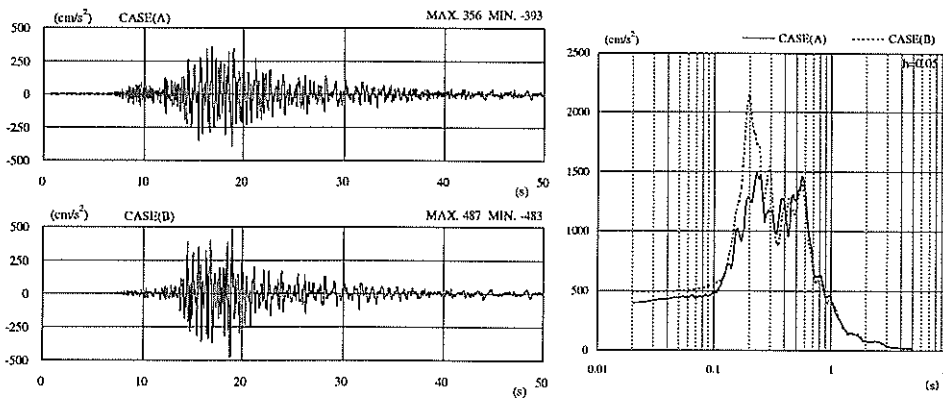

(a) Acceleration Time Histories (b) Response Spectra

Fig.15 Response of Roof